Mo doped vanadium oxide nanotubes: microstructure and electrochemistry

Li-Qiang Mai [*], Wen Chen [*], Qing Xu, Jun-Feng Peng, Quan-Yao Zhu

Institute of Materials Science and Engineering, Wuhan University of Technology, Luoshi Road 122, Wuhan 430070, Hubei, PR China

Abstract

Mo doped vanadium oxide nanotubes (VONT) were prepared via a rheological phase reaction followed by self-assembling process and were heated at 400 °C in an inert atmosphere. The nanotubes were characterized by SEM, HRTEM, XRD, Raman spectroscopy, electrochemical investigation, etc. In contrast to the undoped VONTs, the interlayer distance between oxide layers in the $(V_{0.99}Mo_{0.01})_xONTs$ increases owing to replacement of some V in nanotubes by Mo with a larger ionic radius, resulting in a shorten diffusion length of Li ions and an improved electrochemical performance. Moreover, this study reveals that the electrochemical performance of $(V_{0.99}Mo_{0.01})_xONTs$ is further enhanced by removing the residual organic template by heating in an inert atmosphere.
© 2003 Elsevier B.V. All rights reserved.

1. Introduction

Mo doped vanadium oxides have found a wide range of applications because of their selective oxidation as well as the unique interaction between V_2O_5 and MoO_3 owing to the similarity of ionic radii and the structures in their highest oxidation state [1–3]. These similarities enable the formation of substitutional solid solutions with different oxidation states of cations [2,4]. Nanotubes with one-dimensional structures attract much scientific interests for electrochemical insertion because they offer four different contact regions, namely, the tube ends, the inner and outer wall surfaces as well as the inter-walls spaces. Moreover, they can provide electrolyte-filled channels for faster transport of the ions to the insertion sites [5]. In the present work, Mo doped vanadium oxide nanotubes (VONT) were prepared by modified sol–gel process from layered oxide precursor and organic molecules as structure-directing templates and then heated in an inert atmosphere. The nanotubes were characterized by scanning electron microscopy (SEM), transmission electron microscopy (TEM), X-ray diffraction (XRD), Raman spectroscopy, electrochemical investigation, etc. Experiments are performed in order to study the effect of Mo doping and heat treatment on the structure and electrochemical performance of vanadium oxide nanotubes.

---

[*] Corresponding authors. Fax: +86-27-87642079.
  E-mail addresses: chenw@public.wh.bb.cn (W. Chen); mlq518@hotmail.com (L.-Q. Mai).

2. Experimental

The Mo doped VONTs were prepared via a rheological phase reaction followed by self-assembling process as previously described [6]. V_2O_5, MoO_3 and hexadecylamine were mixed in the molar ratio $(0.5–0.5x):x:0.5$ ($x = 0$, 0.01, 0.05, 0.09, 0.10) in distilled water and the mixture stirred for 48 h in air. The resulting rheological suspension was transferred into a Teflon-lined autoclave with a stainless steel shell. The autoclave was kept at 180 °C for about a week. The final black product was washed with distilled water and dried at 80 °C for 8 h. The dried products were heated in argon at 400 °C for 1.5 h to remove the residual organics in the nanotubes [5].

XRD experiments were done on a D/MAX-III X-ray diffractometer with Cu-Kα radiation and graphite monochrometer. SEM images were attained using a JSM-5610LV scanning electron microscope at 80 kV. HRTEM image was taken in a JEOL JEM-2010FEF microscope operated at 200 kV. The elemental analyses were performed according to [10]. The Raman spectra were taken on a Renishaw RM-1000 laser Raman microscope system. Excitation was with a 40 mW 514.5 nm Ar-ion laser (amount of power on sample is about 5 mW). Both the spectral resolution and the accuracy in the Raman shift are estimated to be $\sim 2 \text{ cm}^{-1}$. The cathode preparation and the test cell were similar to as described in [5]. Li metal was used as the anode. The test cells containing 1 M $LiPF_6$-EC-DEC (1:1 volume ratio) were usually charged to 3.9 V and discharged to 1.4 V at a 0.15 C rate. The experimental accuracy in the discharge capacity measurements is ± 1 mAh/g.

3. Results and discussion

The morphology and microstructure of the products were observed by SEM and HRTEM technique. Fig. 1 shows the SEM images of the sample with Mo doping level varying in the range of 0–10 mol%. It is found that the doping level have great influence on formation and morphology of vanadium oxide nanotubes. For undoped sample, VONTs are frequently grown together in

the form of bundles. The nanotube length can range from 2 to 8 μm. The diameter ranges from 30 to 100 nm. For the Mo doped sample, interestingly, it is found that the nanotube length and diameter decrease with increase of Mo doping level (less than 10 mol%). However, when the Mo doping content is equal to or exceed 10 mol%, the products attained are lamellar composites of oxides and template instead of VONTs, as shown in Fig. 1e. Fig. 2 shows that the HRTEM images of the undoped VONTs and the VONTs with Mo doping content of 1 mol%, which indicates that both of them have a tubular morphology and multiwalled structure. It should be noted that the distance between the oxide layers increases from 2.88 nm of undoped VONTs to 2.93 nm of VONT with Mo doping content of 1 mol%, which is considered to be due to the replacement of V in vanadium oxide nanotubes by Mo with a larger ionic radius [2]. The increase of interlayer distance results in improved Li insertion capacity and cycling capacity. This result is confirmed by the electrochemical test results below. This change in nanotube length implies that the Mo doping process alters the growth kinetics of VONTs [7]. For the heated $(V_{0.99}Mo_{0.01})_x$NTs, the interlayer distance is 1.55 nm and much less than that of either the undoped VONT or the unheated $(V_{0.99}Mo_{0.01})_x$NTs, which can be attributed to the removal of the residual organic template in the nanotubes [6]. The VONTs, $(V_{0.99}Mo_{0.01})_x$NTs and heated $(V_{0.99}Mo_{0.01})_x$NTs will be as the objects to study the influence of Mo doping and heat treatment on the microstructure and electrochemical performance, whose elemental composition and layer distance are listed in Table 1.

XRD measurements were performed on the prepared nanotubes to assess the overall phase structure. Fig. 3 shows the XRD patterns of the VONTs, $(V_{0.99}Mo_{0.01})_x$ONTs and heated $(V_{0.99}Mo_{0.01})_x$ NTs. It can be seen that there are not significant differences among them and two set of diffraction patterns are observed in each of them: the *00l* one corresponding to a well-ordered layer structure and *hk0* one corresponding to the two dimensional structure of the $V(Mo)O_x$ layers which form the walls of the nanotubes, which confirms that Mo atoms enter the crystalline lattice of va-
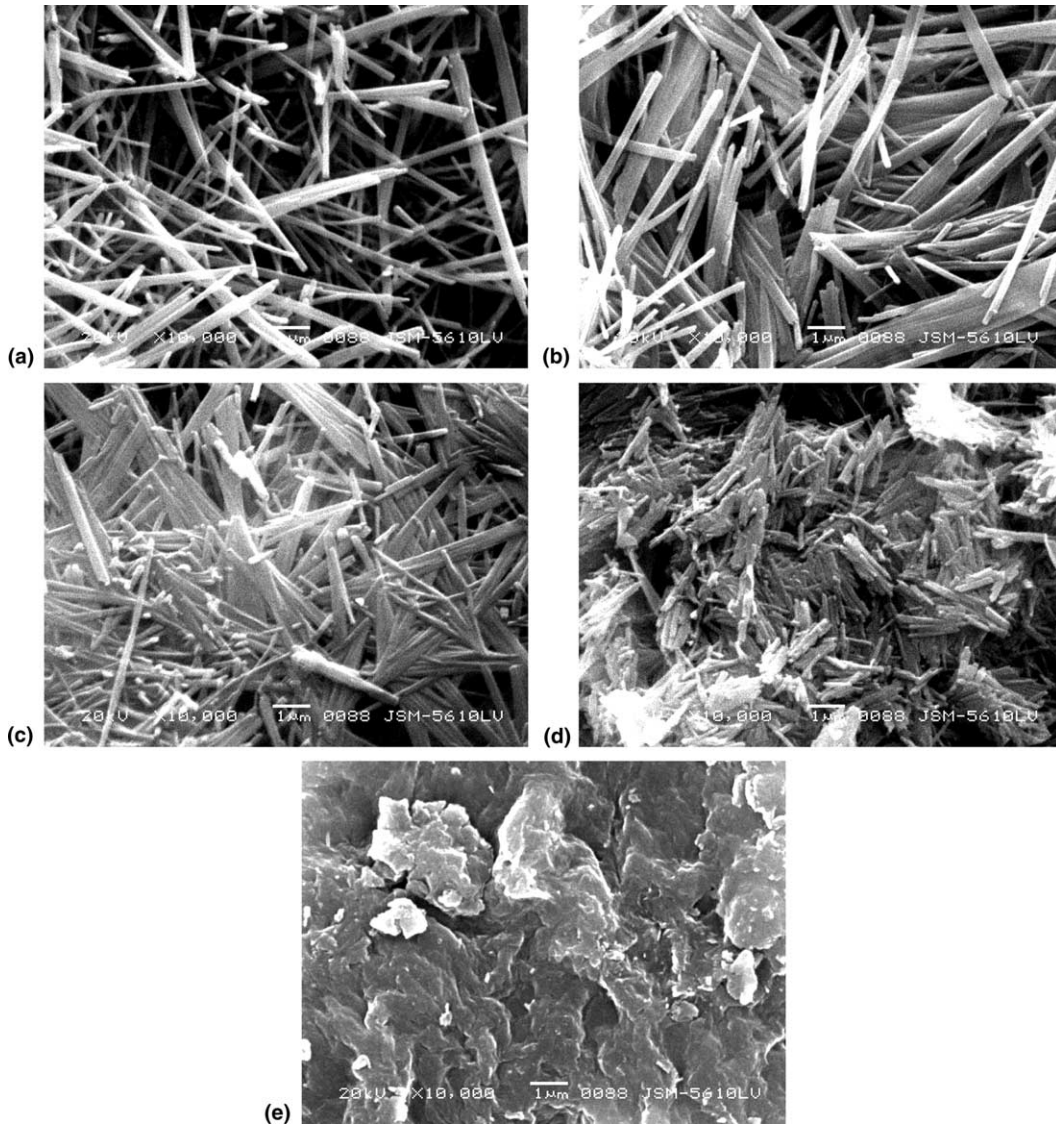
Fig. 1. SEM images of the samples with different Mo–doping content: (a) 0 mol%, (b) 1 mol%, (c) 5 mol%, (d) 9 mol% and (e) 10 mol%.

nadium oxide layer in the nanotubes in the form of a solid solution [8,9]. However, in contrast with the undoped sample, there is a noticeable shift of the 0 0 1 peak toward lower diffraction angle for the Mo doped sample corres- ponding to increase of the interlayer distance from 3.35 to 3.40 nm, which is consistent with above HRTEM result. Although the ED and XRD data coincide regarding the characteristic reflections caused by the structure within the layers, there is a certain discrepancy between the d values of the 0 0 1 reflections corresponding to the layer distance (Table 1). The d values from the XRD data are always larger than those determined by electron diffraction. This deviation might be due to a partial rearrangement of the flexible, paraffin-like arrangement of template molecules between the layers under the influence of the electron beam and to an occasional loss of
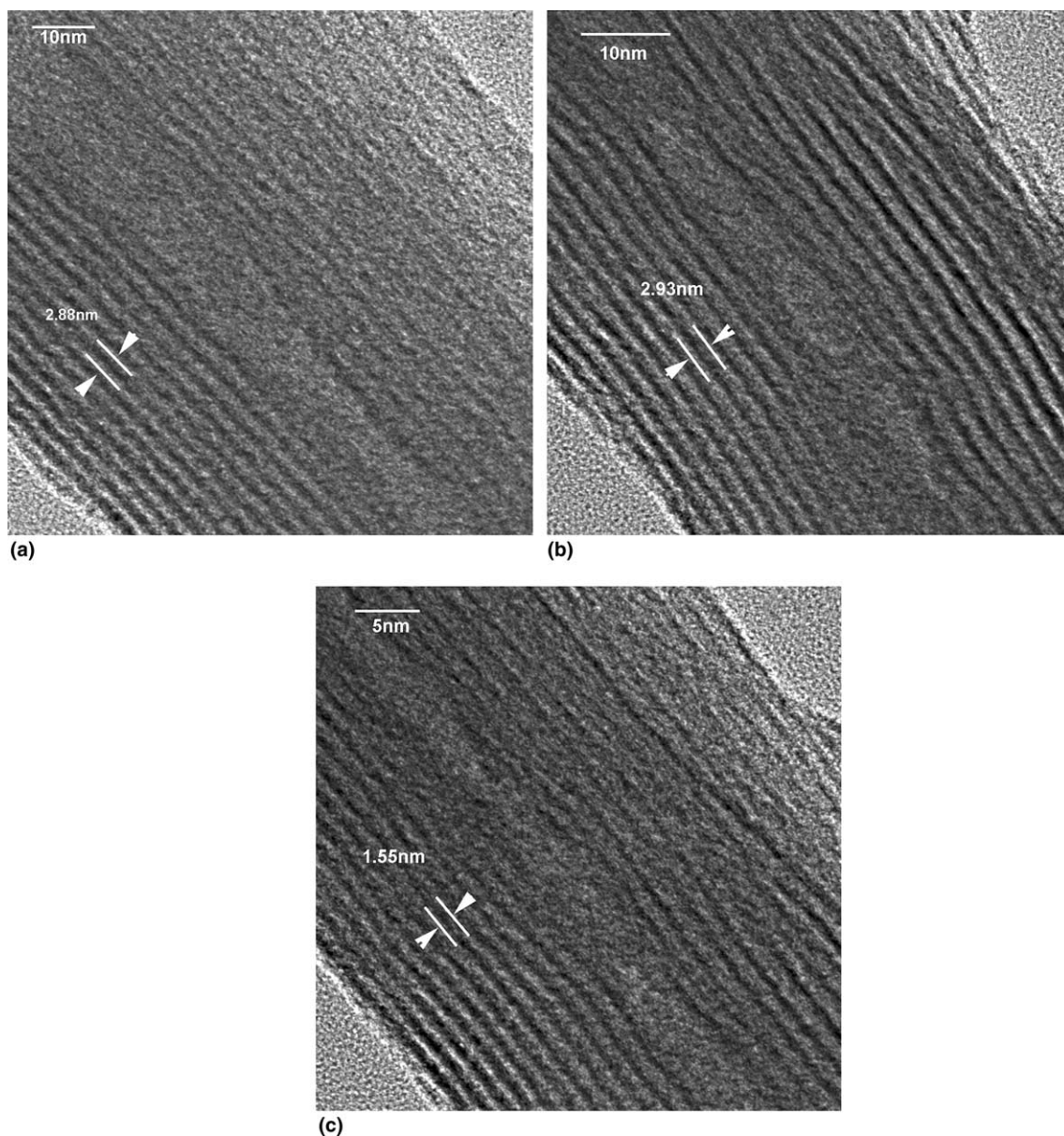
Fig. 2. The HRTEM images of VONT (a), $V_{0.99}Mo_{0.01}ONT$ (b) and heated $V_{0.99}Mo_{0.01}ONT$ (c).

template molecules under the high vacuum conditions [10]. Meanwhile, it is can be found that a in 2D tetragonal cell increases from 0.615 to 0.623 nm [10]. The changes for interlayer and a can also be attributed to the replacement of V in vanadium oxide nanotubes by Mo with a larger ionic radius. Interestingly, heat treatment results in drastic reduction of the interlayer distance to 1.55 nm which
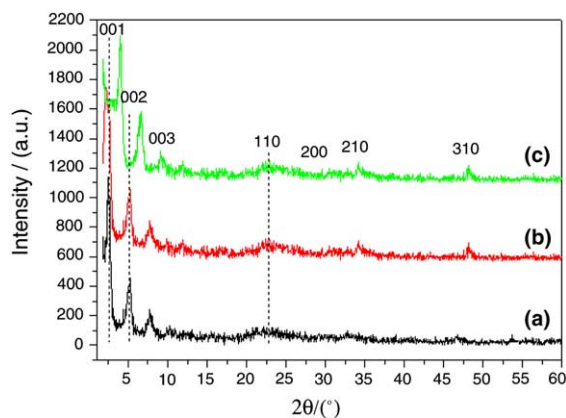
is clearly due to the removal of organic template between oxide layers in the nanotubes. The $hk0$ reflections due to the vanadium oxide sheets remain at the same positions showing that the structure of the layers remains the same.

Raman-scattering measurements were used to examine the microstructure of VO_x–NTs. The Raman spectra of the VONTs, $(V_{0.99}Mo_{0.01})_x$NTs
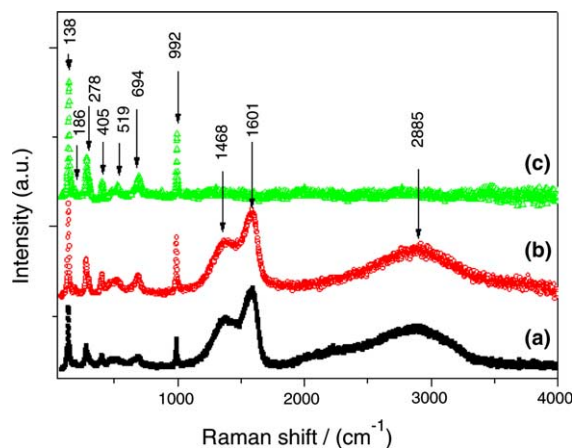
Table 1
Elemental composition and layer distance of VONT, $V_{0.99}Mo_{0.01}ONT$ and heated $V_{0.99}Mo_{0.01}ONT$

Sample	Composition	Interlayer distance (nm)		a (nm)
		XRD	ED	
VONT	$V_{1.00}O_{2.46}(C_{16}H_{36}N)_{0.26}$	3.35	2.88	0.615
$V_{0.99}Mo_{0.01}ONT$	$V_{0.99}Mo_{0.01}O_{2.45}(C_{16}H_{36}N)_{0.27}$	3.40	2.93	0.623
Heated $V_{0.99}Mo_{0.01}ONT$	$V_{0.99}Mo_{0.01}O_{2.46}$	1.56	1.55	0.622

Fig. 3. XRD patterns of VONT (a), $V_{0.99}Mo_{0.01}ONT$ (b) and heated $V_{0.99}Mo_{0.01}ONT$ (c).

Fig. 4. Raman spectra of VONT (a), $V_{0.99}Mo_{0.01}ONT$ (b) and heated $V_{0.99}Mo_{0.01}ONT$ (c).

and heated $(V_{0.99}Mo_{0.01})_xNTs$ are shown in Fig. 4. For comparison, Table 1 give Raman peak frequencies and attributions of phonons in vanadium oxide nanotubes and bulk V_2O_5. It is shown that the Raman peaks at 285, 305, 406, 483, 528, 702, 996 cm^{-1} have a red shift of less than 10 cm^{-1}, which should be attributed to the quantum confinement effect (QCE) [11]. However, the Raman peaks at 285 cm^{-1} have a great red shift of 37 cm^{-1}, which can be associated with the structural defect effects and Fröhlich interaction in nanotubes [12]. For the VONTs and $(V_{0.99}Mo_{0.01})_xNTs$, the Raman peaks at 2885, 1601 and 1468 cm^{-1} can be unambiguously assigned to the presence of residual organic template in the structure [13,14]. The intensity of these peaks disappears after heat treatment, which suggests that the residual organic template has been removed while the structures of vanadium oxide nanotubes are not destroyed because there are no noticeable change for the peaks between 100 and 1000 cm^{-1} corresponding to the various (group) vibrations of M–O type (M=V or Mo), which confirms the results of HRTEM and XRD (see Table 2).

Electrochemical investigations were performed to study the effect of Mo doping and heat treatment on electrochemical performance of vanadium oxide nanotubes. Fig. 5 shows the discharge capacities of the VONTs, $(V_{0.99}Mo_{0.01})_xONTs$ and

Table 2
Raman peak frequencies and attributions of phonons in vanadium oxide nanotubes and bulk V_2O_5

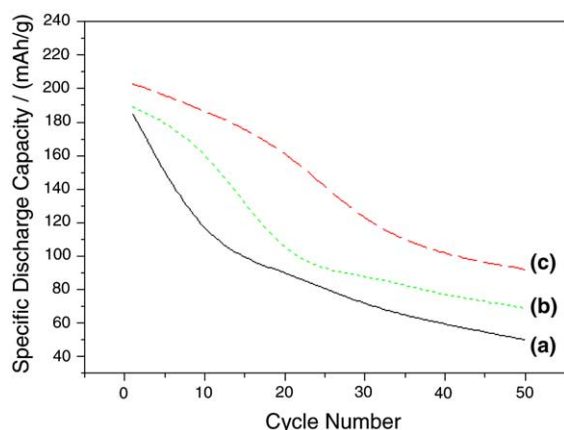| VONT (cm^{-1})	V_2O_5 (cm^{-1})	Attribution
96	104	$\delta(O_2V_2)n$
138	146	$\delta(O_2V_2)n$
186	198	$\delta(O_2V_2)n$
278	285	$\delta(O-V)$
303	305	$\delta(O-V_3)$
405	406	$\delta(O-V)$
482	483	$\delta(O-V_2)$
519	528	$v(O-V_3)$
694	702	$v(O-V_2)$
876	913	$v(O-V)$
992	996	$v(O-V)$

Fig. 5. The specific discharge capacity of VONT (a), $V_{0.99}Mo_{0.01}ONT$ (b) and heated $V_{0.99}Mo_{0.01}ONT$ (c).

heated $(V_{0.99}Mo_{0.01})_xONTs$ as a function of cycle number. It is clearly shown that the first discharge capacity of $(V_{0.99}Mo_{0.01})_xNTs$ (189 mAh/g) is higher than that of the undoped VONTs (185 mAh/g). Meanwhile, the former exhibits better cycling properties than the latter. The high electrochemical performance of the Mo–doped VONTs is assumed to be due to large interlayer distance and short diffusion length of Li ions compared to the undoped one [15,16]. Further study about physicochemical mechanisms induced by Mo doping is underway. Notably, in contrast to VONTs and $(V_{0.99}Mo_{0.01})_xONTs$, the heated $(V_{0.99}Mo_{0.01})_xONTs$ have higher first discharge capacity (203 mAh/g), which is because the removal of the organic allows for insertion and extraction of more lithium ions. Moreover, it is found that the heated $(V_{0.99}Mo_{0.01})_xNTs$ exhibits better cycling property than that of the VONTs and $(V_{0.99}Mo_{0.01})_xNTs$. We propose that the $(V_{0.99}Mo_{0.01})_xNTs$ after heat treatment have more stable microstructure and become more tolerant to repeated charge/discharge.

4. Conclusions

For the first time it is found that the tubular morphology of Mo doped vanadium oxides can be formed under the condition of the Mo doping content of less than 10 mol%. The VONTs with Mo doping content of 1 mol% have better electrochemical performance than that of the undoped ones. The residual organic between transition metal oxide layers in the nanotubes can be removed by heating in an inert atmosphere, which results in an enhanced cycling properties.

References

[1] L. Philippe, T. Christophe, Solid State Sci. 4 (2002) 217.
[2] P. Jin, S. Tanemura, Thin Solid Films 281–282 (1996) 239.
[3] G.T. Chandrappa, N. Steunou, J. Livage, Nature 416 (2002) 702.
[4] M. Demeter, M. Neumann, A.V. Postnikov, V.M. Cherkashenko, V.R. Galakhov, E.Z. Kurmaev, Surf. Sci. 482–485 (2001) 708.
[5] S.T. Lutta, A. Dobley, K. Ngala, S. Yang, P.Y. Zavalij, W.S. Whittingham, Mat. Res. Soc. Symp. Proc. 703 (2002).
[6] L.Q. Mai, W. Chen, Q. Xu, Q.Y. Zhu, C.H. Han, J.F. Peng, Solid State Commun. 126 (2003) 541.
[7] N. Yu, T.W. Simpson, P.C. Mclntyre, M. Nastasi, I.V. Mitchell, Appl. Phys. Lett. 67 (1995) 924.
[8] J. Cho, Y.J. Kim, T.J. Kim, Chem. Mater. 13 (2001) 18.
[9] J. Cho, Y.J. Kim, B. Park, J. Electrochem. Solid State 4 (2001) A159.
[10] F. Krumeich, H.J. Muhr, M. Niederberger, F. Bieri, B. Schnyder, R. Nesper, J. Am. Chem. Soc. 121 (1999) 8324.
[11] W. Han, S.S. Fan, Q. Li, Phys. Lett. 265 (1997) 374.
[12] K. Huang, B.F. Zhu, Phys. Rev. B 38 (1988) 2183.
[13] L.A.E. Batista de Carvalho, L.E. Lourenço, M.P.M. Marques, J. Mol. Struct. 482 (1999) 639.
[14] W.B. Fischer, H.H. Eysel, J. Mol. Struct. 415 (1997) 249.
[15] D. Imammura, M. Miyayama, Solid State Ionics 161 (2003) 173.
[16] S. Castro-Garcia, A. Castro-Couceiro, M.A. Senaris-Rodriguez, F. Soulette, C. Julien, Solid State Ionics 156 (2003) 15.